Dental Materials xxx (xxxx) xxx

Contents lists available at ScienceDirect

Dental Materials

journal homepage: www.elsevier.com/locate/dental

Developing a novel glass ionomer cement with enhanced mechanical and chemical properties

Ollie Yiru Yu *, Kelsey Xingyun Ge, Christie Ying-Kei Lung, Chun-Hung Chu

Faculty of Dentistry, The University of Hong Kong, Hong Kong Special Administrative Region

ARTICLE INFO

Keywords:
Poly(vinylphosphonic acid)
45S5 nanosilver bioactive glass
Glass ionomer cement
Mechanical properties
Dental caries
Caries prevention

ABSTRACT

Objective: To develop a novel glass ionomer cement (NGIC) with enhanced mechanical and chemical properties and assess its biocompatibility, mechanical strength, and ion release.

Methods: Nanosilver doped bioactive glass (NanoAg BAG) was synthesized by sol-gel method and characterized by scanning electron microscopy with energy-dispersive X-ray spectroscopy and transmission electron microscopy. The NanoAg BAG, together with poly(vinylphosphonic acid) (PVPA), alumino-fluorosilicate glass and poly-acrylic acid were used to synthesize NGIC. The optimal PVPA concentration for NGIC was determined by PVPA modified GIC's biocompatibility and mechanical properties and used to prepare NGIC specimens. NGIC specimens with NanoAg BAG at 0%, 1%, 2%, and 5% were allocated into Groups NGIC0, NGIC1, NGIC2, and NGIC5, respectively. The biocompatibility, surface morphology, elemental composition, surface topography, chemical properties, compressive strength, diametral tensile strength, and ion release of the NGIC were assessed. A conventional glass ionomer cement (GIC) was used as a control.

Results: A granular BAG with nano silver particles attached on its surface were found, indicating the successful synthesis of NanoAg BAG. PVPA at 10% presented the best effect in enhancing the biocompatibility and mechanical properties of PVPA modified GIC and was used to prepare NGIC specimens. NGIC1 showed similar biocompatibility, surface morphology and topography to GIC. Chemical properties results showed that NGICs showed the same adsorption peaks to GIC. The compressive strength (mean±SD in MPa) was 168.1 ± 29.7, 205.5 ± 29.5, 221.8 ± 46.8, 216.6 ± 59.3 and 167.7 ± 36.4, and the diametral tensile strength (mean±SD in MPa) was 14.1 ± 1.7, 18.3 ± 4.9, 21.2 ± 2.2, 17.2 ± 3.8 and 13.3 ± 3.3 for GIC, NGIC0, NGIC1, NGIC2 and NGIC5 respectively. NIGC0, NGIC1 and NGIC2 showed higher compressive and diametral tensile strength than GIC ($p < 0.01$). NGIC2 and NGIC5 showed higher release of fluoride, calcium, phosphate and silver ion than GIC and NGIC0 ($p < 0.05$).

Conclusion: A biocompatible NGIC with enhanced mechanical properties were developed. It presented enhanced fluoride, calcium, phosphate and silver ion release compared to conventional GIC.

1. Introduction

Glass-ionomer cements (GIC), or glass polyalkenoate cements, are dental materials commonly used as luting cements, dental sealants and restorative materials [1]. GIC offers several advantages including chemical adhesion to tooth tissue, a similar thermal coefficient to dental hard tissue and sustainable fluoride release [2]. These benefits result in GIC's simple operative procedures, low shrinkage rate after setting, and inhibition to secondary caries. Due to its favorable caries-preventive properties, World Health Organization (WHO) included GIC in the WHO Model List of Essential Medicine in 2021 [3].

Untreated dental caries, a widespread chronic oral disease, affects 2.5 billion adults and 573 million children [4]. The philosophy for caries management have been evolving towards minimal intervention dentistry (MID), emphasizing remineralization of dental hard tissue, optimal preventive measures and minimally invasive operative treatment [5]. Managing dental caries with GIC is a promising stategy embrasing the MID philosophy. It releases fluoride, which prevents deminealisation, promotes remineralisation and inhibits the bacteria growth of the carious teeth. GIC can be employed for caries prevention and presents better caries preventive effect than other dental materials. It is also suitable to be applied in cavities prepared with selective caries

* Correspondence to: Faculty of Dentistry, The University of Hong Kong, 34 Hospital Road, Hong Kong Special Administrative Region.
E-mail address: ollieyu@hku.hk (O.Y. Yu).

https://doi.org/10.1016/j.dental.2024.05.019
Received 7 August 2023; Received in revised form 12 May 2024; Accepted 13 May 2024

removal strategies and promotes remineralisation of affected dentine in minimally invasive operative treatment [6,7].

However, GIC demonstrates low fracture toughness and flexural strength, which can lead to microleakage or fractures when it is used for restorations [8]. Consequently, GIC is not suitable for stress-bearing areas and has a generally shorter clinical longevity compared to other types of restoration [9]. To enhance the performance of GIC, substantial efforts have been dedicated to formulating improved version. Nevertheless, apart from the development of resin-modified formulations of GIC, the reports on the development of new formulated GIC were minimal [10]. Although resin-modified GIC demonstrated improved mechanical strength compared to conventional GIC, its polymerization shrinkage and moisture sensitivity increased [11]. Another concern was the diminished fluoride release activity of resin-modified GIC due to the introduction of the resin system, which reduced its caries preventive effects [12]. Previous clinical studies have revealed a high failure rate and a short lifespan of GIC restorations, which was mainly due to the fracture of GIC restorations or recurrent caries around restorations. The reasons for the clinical failure of GIC suggests that the mechanical strength, antimicrobial effect and remineralising effect of conventional GIC are unsatisfactory and should be improved [8,9].

Poly (vinylphosphonic acid) (PVPA) has potential in enhancing the mechanical strength of GIC [13]. Conventional GIC consists of fluoroaluminosilicate glass powder and polyacrylic acid solution [14]. PVPA is the phosphorus analogue to polyacrylic acid. It is a macromolecule with a high density of phosphonic acid units on its polymer backbone [15,16]. PVPA is more reactive than polyacrylic acid [17]. It forms more and stronger binding with the metal ions such as calcium and aluminum in the fluoroaluminosilicate glass, which might enhance the mechanical strength of the material [18]. PVPA is water-soluble. Khouw-Liu reported that the PVPA-based cement had a good resistance to water. An early exposure to water did not affect its mechanical strength [19]. Therefore, the addition of PVPA might improve the mechanical properties of GICs.

Bioactive glass (BAG) is a type of biomaterial that possesses limited antibacterial and remineralizing properties [20]. 45S5 Bioglass is a bioactive glass specifically composed of 45 wt% SiO_2, 24.5 wt% CaO, 24.5 wt% Na_2O, and 6.0 wt% P_2O_5 [21]. The United States Food and Drug Administration (FDA) has approved 45S5 Bioglass for clinical applications [22]. 45S5 Bioglass has excellent biocompatibility, and has been widely used as a clinical bone filling material due to its regenerate bone ability [23]. In dentistry, 45S5 bioglass is used in dental air polishing or caries removal procedures to improve the remineralization of tooth hard tissue [24]. BAG has been shown to exhibit antimicrobial properties, although not at a particularly high level [25]. Silver nanoparticles are broad-spectrum antimicrobial agents that can be added to BAG to enhance its antimicrobial effect [26,27]. Silver nanoparticles incorporated BAG (NanoAg BAG) can release silver to inhibit the growth of oral bacteria and calcium and phosphate ions to promote remineralisation [28]. The addition of NanoAg BAG to GIC might potentially improve GIC's antimicrobial and remineralising effects by improving GIC's chemical properties, such as silver, calcium and phosphate ion release. Therefore, we aimed to develop a novel glass ionomer cement (NGIC) with enhanced mechanical and chemical properties and assess its biocompatibility, mechanical strength, and release of fluoride, calcium, phosphate and silver ions.

2. Materials and methods

2.1. Synthesis of 45S5 bioactive glass loaded with silver nanoparticles (NanoAg BAG)

The synthesis of NanoAg BAG (3 mol% Ag, 43.1 mol% SiO_2, 24.4 mol % Na_2O, 26.9 mol% CaO, 2.6 mol% P_2O_5) by sol-gel method was modified from a previous study [29]. A 7.31 g of tetraethyl orthosilicate (TEOS) was added to 1 M nitric acid with a molar ratio of H_2O: TEOS = 18: 1. The mixture was stirred for 2 h until a clear sol was formed. Next, 0.77 g of triethyl phosphate and 5.17 g of calcium nitrate were added, followed by 3.38 of sodium nitrate and finally, a 0.42 g of silver nitrate. The mixture was stirred until all chemicals dissolved and then heated to 60ºC for 24 h. The gel formed was dried overnight at 80 °C. The dried gel was calcined at 700 °C for 3 h. The collected solid was ground to obtain a fine powder.

2.2. Characterization of NanoAg BAG

We used Scanning electron microscopy (SEM, Hitachi S-4800 FEG Scanning Electron Microscope; Hitachi, Tokyo, Japan) to examine the morphology of the NanoAg BAG powder. Energy-dispersive X-ray spectroscopy (EDS) under the SEM was used to analyze the elemental composition of the NanoAg BAG powder. Prior to analysis, the NanoAg BAG powder was sputter-coated with 80% Pt and 20% Pd. Transmission electron microscopy (TEM, FEI Tecnai G2 20 Scanning Transmission electron microscopy, FEI, Oregon, USA) with energy dispersive X-ray element mapping were employed to characterize the morphological and compositional properties of the powder.

2.3. Optimal PVPA concentration for NGIC synthesis

We used a commercially available poly(vinylphosphonic acid) (PVPA, Polysciences, Inc, USA) to synthesize PVPA modified GIC (PVPA-GIC). The optimal PVPA concentration for NGIC was determined by assessing the mechanical properties of PVPA-GIC with different ratios of PVPA incorporated and subsequently used for the preparation of NGIC specimens. PVPA-GIC specimens with PVPA solid at 1%, 5%, 10% and 20% weight percentage were prepared and allocated into Groups 1% PVPA, 5% PVPA, 10% PVPA and 20% PVPA, respectively. Conventional GIC (GC Corporation, Tokyo, Japan) was used as a control. The composition of the experimental materials was shown in Table 1.

The PVPA-GIC and GIC specimens were prepared by manually mixing liquid with alumino-fluorosilicate glass powder in a 3.6:1 (w/w) ratio. The biocompatibility, compressive strength and diametral tensile strength of the specimens were assessed.

2.3.1. Biocompatibility of NGIC

We evaluated the biocompatibility of the NGICs specimens with cell cytotoxicity tests on human gingival fibroblast cells (HGFs) following the ISO 7405:2018 standard. Circular specimens with a diameter of 5 mm and a height of 2 mm were prepared using a Teflon mold. HGFs (3×10^3) were inoculated (or seeded) onto the surface of the specimens in a 96-well plate. In control group, the well containing culture medium with HGFs (3×10^3). In blank group, the well containing culture medium without HGFs. The proliferative potential of HGFs was determined by the Cell Counting Kit-8 (CCK-8, Apexbio, MA, USA) assay. After 1, 3, 5, and 7 days of coculture, HGFs were treated with CCK-8 agents at 37 °C for 2 h, and the optical density (OD) at 450 nm was measured using a microplate reader. Six specimens from each group at each timepoint were evaluated. The total number of specimens were 24 for each group. The experiment was repeated for 3 times.

Table 1
Composition (wt%) of the experimental glass ionomer cements (GICs) with poly (vinylphosphonic acid)(PVPA).

Group	Experimental GIC	Silicate glass	Poly-acrylic acid / PVPA
GIC	GIC (conventional)	100	100
1% PVPA	GIC with 1% PVPA	100	99 /1
5% PVPA	GIC with 5% PVPA	100	95 / 5
10% PVPA	GIC with 10% PVPA	100	90 / 10
20% PVPA	GIC with 20% PVPA	100	80 / 20

2.4. Testing of mechanical properties

We evaluated the compressive strength and diametral tensile strength of the experimental glass ionomers according to ISO standards (ISO 9917–1:2007). The cylindrical specimens were prepared using Teflon molds with a height of 6 mm and a diameter of 4 mm (n = 6 per group). For assessment of compressive strength, the specimens were stored in water at 37 °C for 24 h. The compressive strength was determined using a universal testing device (Electropuls E3000 Universal Testing System, Instron, MA, USA) with a 3 kN load cell at a crosshead speed of 0.5 mm/min. A load was applied until fracture occurs. For assessment of diametral tensile strength, the specimens (n = 6 per group) were mounted in the universal testing device with cross-head speed of 0.5 mm/min. The diametral tensile strength (MPa) was calculated using the following formula: $(2 \times p)/(\pi \times d \times t)$, where p is the ultimate tensile strength (N), d is the diameter and t is the height.

2.5. Preparation of novel glass ionomer cement (NGIC)

We used the synthesized silver doped bioactive glass (NanoAg BAG) powder to prepare NGIC. NGIC specimens with NanoAg BAG at 0%, 1%, 2% and 5% weight percentage were prepared and allocated into four groups: Conventional GIC served as the control. The composition of each group is shown in Table 2.

The specimens were prepared by manually mixing liquid with silicate glass-powder (alumino-fluorosilicate glass) in a 3.6:1 (w/w) ratio. The biocompatibility, chemical properties, surface properties, mechanical strength and ion release of the NGIC specimens were assessed.

2.6. Biocompatibility

Circular specimens with a diameter of 5 mm and a height of 2 mm were prepared using Teflon mold. The biocompatibility of the NGICs specimens was evaluated through cell cytotoxicity tests on human gingival fibroblast cells (HGFs). The cytotoxicity of NGICs against HGFs was evaluated according to the method described in Section 2.3.1.

2.7. Surface morphology, elemental composition, and roughness

Circular specimens with a diameter of 5 mm and a height of 2 mm were prepared using Teflon mold. The surfaces morphology of NGICs were assessed using a SEM (Hitachi S-4800 FEG Scanning Electron Microscope; Hitachi, Tokyo, Japan). The elemental composition of NGICs was analyzed using EDS under the SEM. Atomic-force microscopy (AFM, Bruker Corporation, Karlsruhe, Germany) was used to evaluate NGICs' surface roughness. The images of NGICs' surface topography were obtained from 20 × 20 μm^2 samples at the scan speed of approximately 1 Hz in the contactless tapping mode. The mean surface roughness values (Ra) were determined for each specimen. Six specimens from each group were evaluate. The total number of specimens were 30 for each test.

Table 2
Composition (wt%) of glass ionomer cements (GICs) with Ag45S5 bioactive glass (NanoAg BAG) and poly(vinylphosphonic acid)(PVPA).

Group	Experimental GICs	Silicate glass / NanoAg BAG	Poly-acrylic acid / PVPA
GIC	GIC (conventional)	100	100
NGIC0	GIC with 10% PVPA	100	90 / 10
NGIC1	10% PVPA + GIC with 1% NanoAg BAG	99 / 1	90 / 10
NGIC2	10% PVPA + GIC with 2% NanoAg BAG	98 / 2	90 / 10
NGIC5	10% PVPA + GIC with 5% NanoAg BAG	95 / 5	90 / 10

2.8. Chemical properties of NGICs

Circular specimens with a diameter of 5 mm and a height of 2 mm were prepared using Teflon mould (n = 6 per group). After setting for 24 h, the chemical structural of the specimens after the setting reaction were determined by Fourier transform infrared spectroscopy (FTIR, UMA 500, Bio-Rad Laboratories, Hercules, CA, USA). FTIR spectra of GIC, NGIC0, NGIC1, NGIC2 and NGIC5 were recorded on a FTIR in the transmission mode with an attenuated total reflection module. All spectra were recorded at a wavelength range from 4000 to 400 cm^{-1}, with the resolution of 4 cm^{-1} and 10 scans.

2.9. Mechanical properties of NGIC

Cylindrical specimens of 6 mm in high and 4 mm in diameter were prepared using a Teflon mold. The specimens (n = 6 per group) were stored in water at 37 °C for 24 h. Compressive strength and diametral tensile strength were evaluated according to the method described in Section 2.3.

2.10. Ion release measurement

The release of fluoride, calcium, phosphate and silver ions of NGIC was evaluated. To investigate the fluoride ion release ability of NGICs, circular specimens with a diameter of 5 mm and a height of 2 mm were prepared using a Teflon mold. The specimens (n = 6 per group) were then immersed in 1 mL of deionized water for 4 weeks. Fluoride concentration in storage solution was measured at different intervals using a fluoride ion-selective electrode (Orion 9609BNWP, Thermo Scientific, Newport, UK) connected to an ion analyser (2700 OAKTON, Eutech Instruments, Singapore). To investigate calcium, phosphate and silver ion release ability of NGICs, the specimens were immersed in 4 mL deionized water for 4 weeks. At defined times, the immersion liquid was exchanged completely. Calcium, phosphate and silver released into the water were measured using an inductively coupled plasma-optical emission spectrometry (ICP-OES, Spectro Arcos, Kleve, Germany).

2.11. Statistical analysis

We analyzed the data using SPSS Statistics 20 (IBM Corporation, Somers, NY, USA). All data were tested for normal distribution using the Shapiro-Wilk test for normality. The data were analyzed by One-way Analysis of Variance. The significance level was set at 95%.

3. Results

3.1. Characterization of NanoAg BAG

Fig. 1 shows the NanoAg BAG granular particles in various magnifications. The EDS spectrum demonstrated that the NanoAg BAG contained a silver peak. Bright-field transmission electron microscopy images of NanoAg BAG displayed the presence of silver-like particles on the surface of BAG (Fig. 2). Elemental mapping showed the distribution of O, Na, Si, P, Ag and Ca elements (Fig. 2). These findings confirm the successful synthesis of NanoAg BAG.

3.2. Optimal PVPA concentration for NGIC synthesis

3.2.1. Biocompatibility of GIC with PVPA

Fig. 3 shows the OD values of the CCK-8 essay with different GIC specimens. GIC with up to 20% PVPA exhibited no difference in biocompatibility with conventional GIC ($p > 0.05$). The addition of PVPA in GIC demonstrated no difference with conventional GIC in biocompatibility tests.

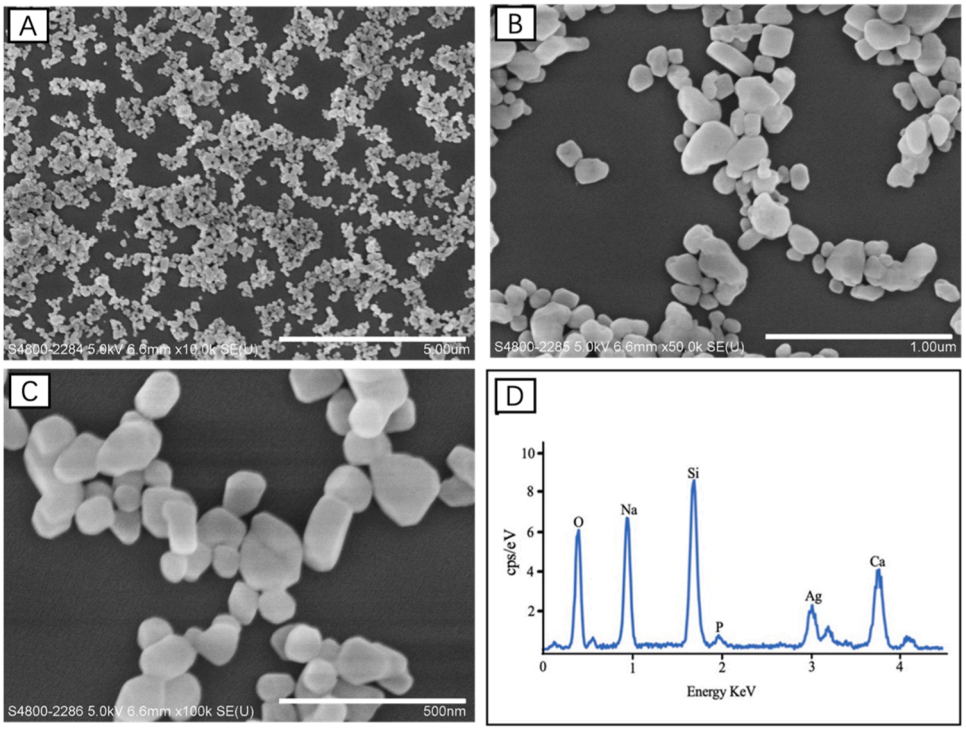

Fig. 1. Scanning electron micrographs and energy-dispersive X-ray spectrum of Ag45S5 bioactive glass (NanoAg BAG). A) 2000 × magnification view of NanoAg BAG showing granular particles. B) 6000 × magnification view of NanoAg BAG. C) 10,000 × magnification view of NanoAg BAG. D) EDS spectrum of NanoAg BAG.

3.2.2. Compressive strength of GIC with PVPA

The mean compressive strength and SD of GIC, 1% PVPA, 5% PVPA, 10% PVPA and 20% PVPA was 160.68 ± 40.37 MPa, 177.34 ± 29.20 MPa, 201.53 ± 39.57 MPa, 216.76 ± 10.03 MPa and 19.06 ± 5.92 MPa, respectively. The 10% PVPA group exhibited significantly higher compressive strength than GIC (Fig. 4A, $*p < 0.05$), while 20% PVPA group showed significantly lower compressive strength than GIC (Fig. 4A, $***p < 0.001$).

3.2.3. Diametral tensile strength of GIC with PVPA

The mean diametral tensile strength (DTS) and SD of GIC, 1% PVPA, 5% PVPA, 10% PVPA and 20% PVPA was 14.14 ± 1.67 MPa, 15.76 ± 1.78 MPa, 16.74 ± 3.32 MPa, 21.46 ± 4.83 MPa and 3.41 ± 1.22 MPa, respectively. Fig. 4B shows DTS of 10% PVPA specimens was higher than conventional GIC specimens ($p < 0.05$), whereas DTS of 20% PVPA specimens is lower DTS than conventional GIC specimens ($p < 0.001$).

3.2.4. Optimal PVPA concentration for NGIC

The 10% PVPA group displayed the highest mechanical strength among all groups. Consequently, 10% PVPA was the optimal concentration and was used for the preparation of NGIC.

3.3. Biocompatibility of NGICs

Fig. 5 the OD values of the CCK-8 essay with various NGIC and GIC specimens. NGIC1 exhibit no significant difference in biocompatibility to GIC after 1, 3, 5 and 7 days ($p > 0.05$). On the day 3, 5 and 7, NGIC2 and NGIC5 showed lower viability of human gingival fibroblasts compared to GIC ($p < 0.05$).

3.4. Elemental composition, surface morphology and roughness of NGICs

3.4.1. Surface morphology

Fig. 6 (left) shows typical surface morphology of the NGIC and GIC specimens under SEM. The surface morphology of NGICs and GIC had no observable difference. The specimen fractured-surface revealed that all specimens possessed an irregular glass-ceramic structure with uneven particle distribution.

3.4.2. Elemental composition

Fig. 6 (right) shows typical spectrum of energy dispersive X-ray (EDS) analysis for the NGIC and GIC specimens. The peaks (from, left to right) found in the spectrum of NGIC1, NGIC2 and NGIC5 were carbon (C), oxygen (O), fluorine (F), sodium (Na), aluminum (Al), silicon (Si), phosphorus (P), silver (Ag) and calcium (Ca). The silver atomic percentage in NGIC1, NGIC2 and NGIC5 groups were 0.20%, 0.38% and 0.55%. Spectrum of GIC and NGIC0 specimens have no silver peak.

3.4.3. Surface roughness

Fig. 7 shows the surface topography of the NGIC and GIC specimens. No observable difference in surface topography was found the specimens in the five groups. The mean and SD of surface roughness values (Ra) of GIC, NGIC0, NGIC1, NGIC2 and NGIC5 were 82.5 ± 12.3, 79.3 ± 9.0 nm, 79.2 ± 17.4 nm, 75.8 ± 19.8 nm and 94.6 ± 11.7 nm, respectively. NGIC5 specimens presented a rougher surface than the specimens in the other four groups ($p < 0.05$).

3.5. Chemical properties of NGICs

Fig. 8 showed the typical FTIR spectra for the NGIC and GIC specimens. In NGIC1, NGIC2 and NGIC5 groups, the adsorption peaks at 940 cm^{-1} and 1030 cm^{-1} are associated with the Si-OH and Si-O-Si stretching vibrations from the fluoroaluminosilcate glass powder component and 45 S silver bioactive glass, and the P = O stretching from PVPA after setting. In NGIC0 group, the adsorption peaks at 940 cm^{-1} and 1030 cm^{-1} are associated with the Si-OH and Si-O-Si stretching vibrations from the fluoroaluminosilcate glass powder component and the P = O stretching from PVPA after setting.

In NGIC0, NGIC1, NGIC2 and NGIC5 groups, the adsorption peak at 1403 cm^{-1} and 1458 cm^{-1} are associated with the C═O symmetric and asymmetric vibrations from the polyacrylic acid liquid component after

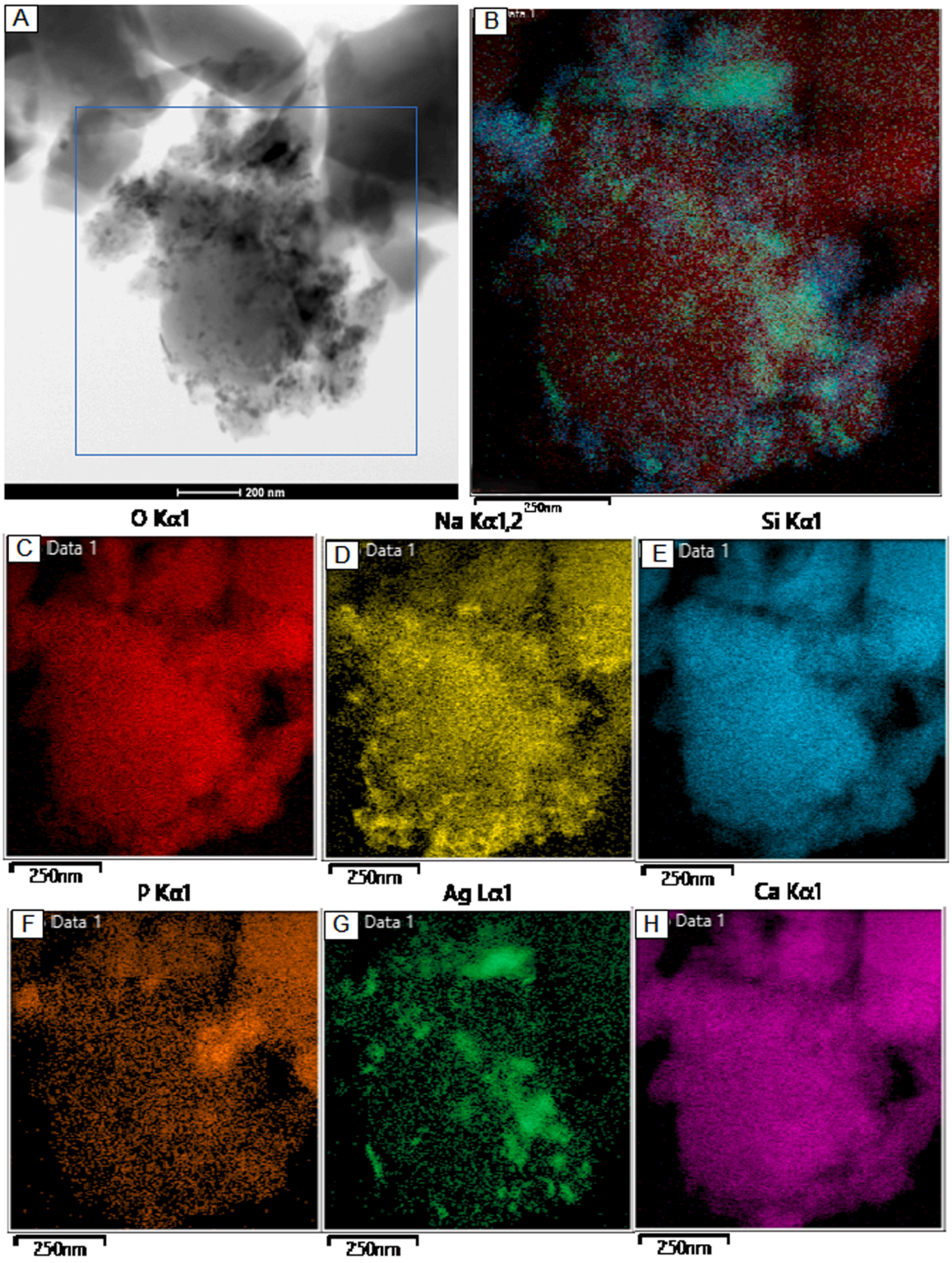

Fig. 2. Transmission electron micrographs and elemental mapping of silver doped 45S5 bioactive glass. A) Bright-field transmission electron micrograph; B) Merge of oxide (O), sodium (Na), silicon (Si), phosphate (P) silver(ag), calcium (Ca) element mapping; C) O element mapping; D) Na element mapping; E) Si element mapping; F) P element mapping; G) Ag element mapping; H) Ca element mapping.

setting. The adsorption peak at 1550 cm^{-1} is associated with the ionized COO- stretching vibration after setting. This is due to the formation of salts of polyacrylic acid (PAA) with Ca^{2+} and Al^{3+} from fluoroaluminosilcate glass powder ($PAA^{-}\_\_Ca^{2+}$ and $PAA^{-}\_\_Al^{3+}$) after setting. The adsorption peak at 1700 cm^{-1} is associated with the C═O carbonyl stretching vibration (COOH) from polyacrylic acid that unionized after setting. The adsorption peaks at 2800 and 2900 cm^{-1} are associated with the asymmetric and symmetric C-H stretching vibrations from polyacrylic acid. The adsorption peak between 3200 and 3500 cm^{-1} is associated with -OH hydroxyl stretching vibration which is due to the crystal network of NGICs and its composite [30,31].

In GIC group, the Si-OH and Si-O-Si stretching vibrations are

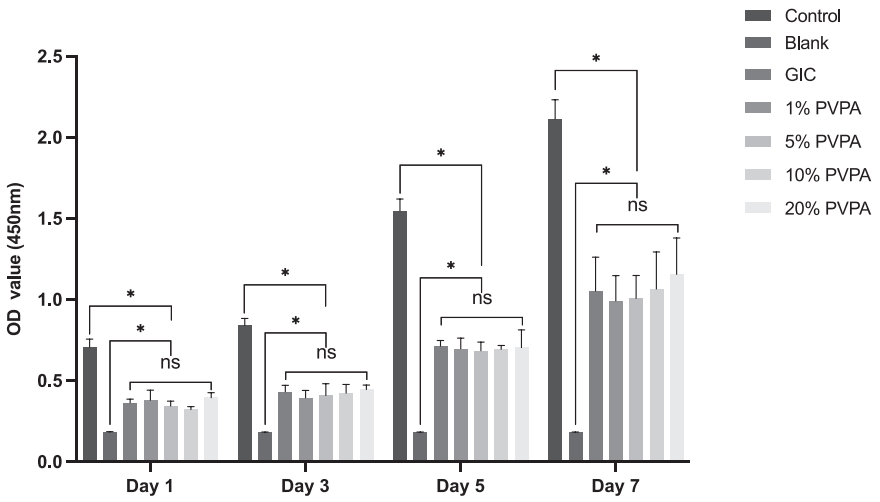

Fig. 3. Human gingival fibroblasts viability (OD value) on the glass ionomer cement (GIC) specimens for 7 days using Cell Counting Kit-8 assay (* $p < 0.05$) (ns $p > 0.05$). *1% PVPA, GIC with 1% poly(vinylphosphonic acid) solid by weight 5% PVPA, GIC with 5% poly(vinylphosphonic acid)solid by weight 10% PVPA, GIC with 10% poly(vinylphosphonic acid)solid by weight. 20% PVPA, GIC with 20% poly(vinylphosphonic acid)solid by weight.*

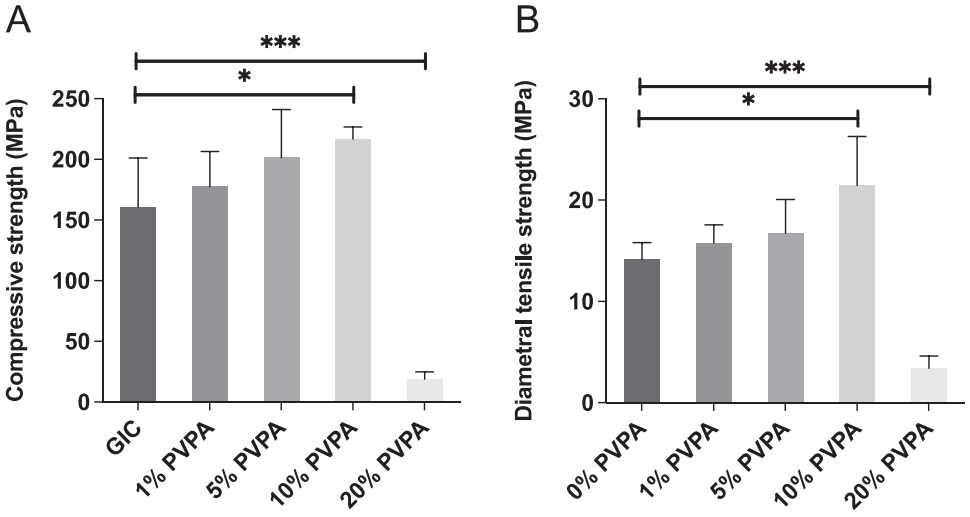

Fig. 4. Compressive strength (A) and diametral tensile strength (B) of the glass ionomer cement specimens (*$p < 0.05$, ***$p < 0.001$). *1% PVPA, GIC with 1% poly (vinylphosphonic acid)solid by weight. 5% PVPA, GIC with 5% poly(vinylphosphonic acid)solid by weight 10% PVPA, GIC with 10% poly(vinylphosphonic acid)solid by weight. 20% PVPA, GIC with 20% poly(vinylphosphonic acid)solid by weight.*

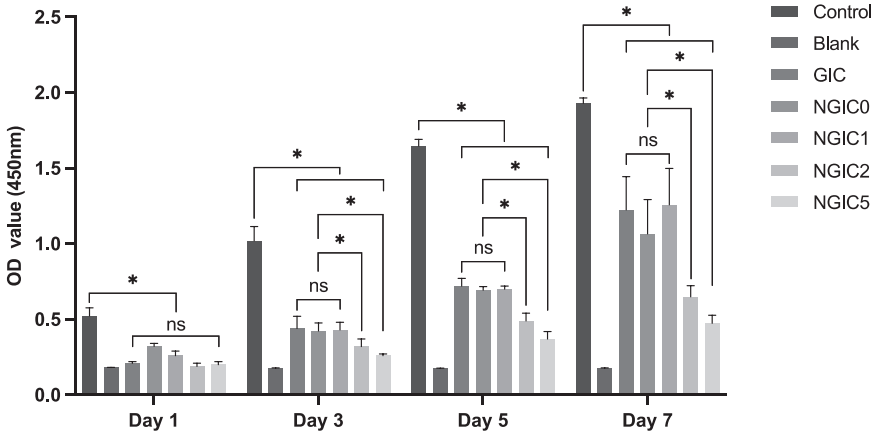

Fig. 5. Human gingival fibroblasts viability (OD value) on glass ionomer cement (GIC) specimens for 7 days using Cell Counting Kit-8 assay (* $p < 0.05$) (ns $p > 0.05$). *NGIC0, GIC with 10% poly(vinylphosphonic acid)(PVPA) solid by weight. NGIC1, GIC with 1% Ag45S5 bioactive glass (NanoAg BAG) and 10% PVPA solid by weight. NGIC2, GIC with 2% NanoAg BAG and 10% PVPA solid by weight. NGIC5, GIC with 5% NanoAg BAG and 10% PVPA solid by weight.*

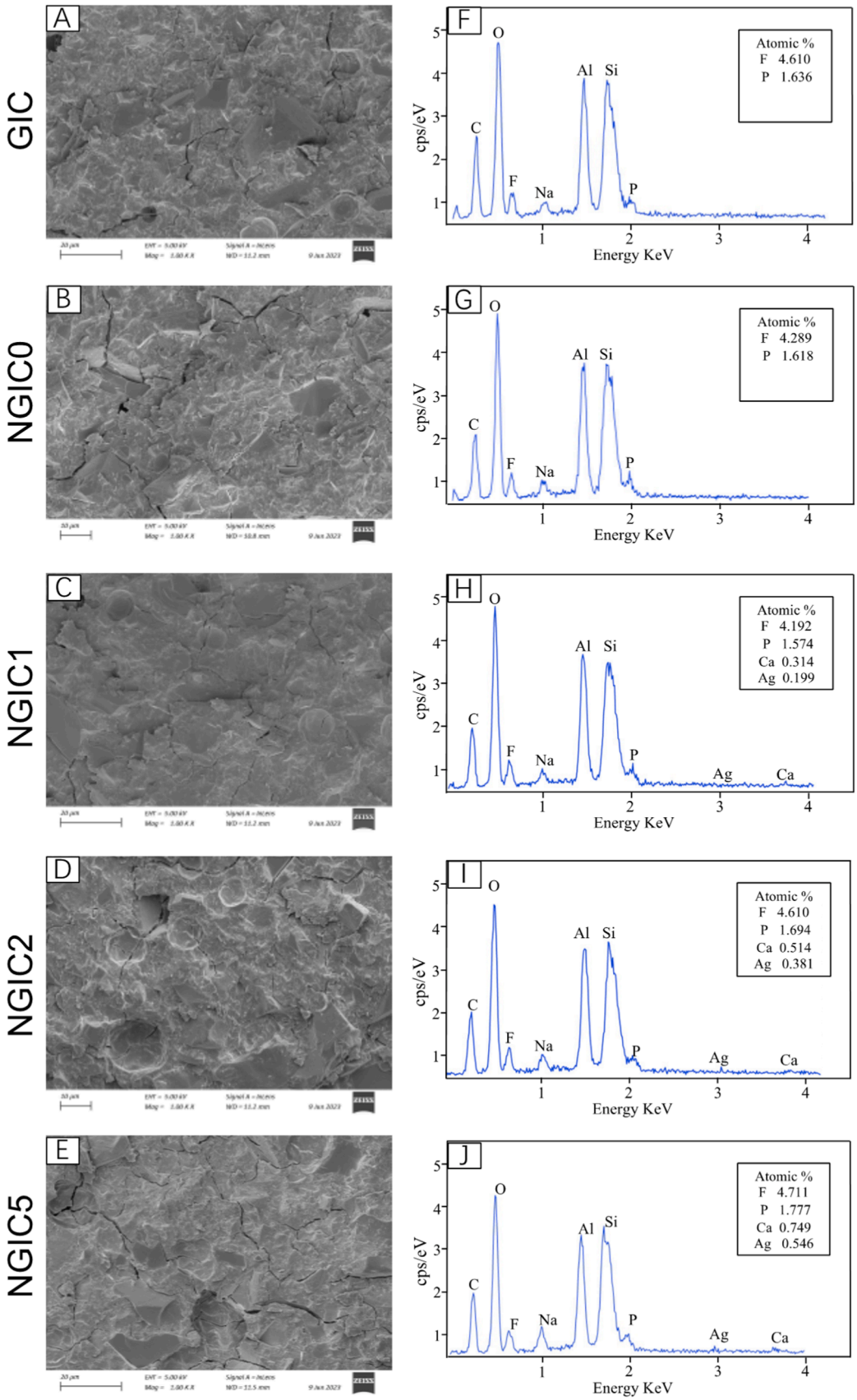

(caption on next page)

Fig. 6. Surface morphology and elemental composition of novel glass ionomer cements (NGICs). Scanning electron micrographs at 1,000x (left) had no observable difference of fracture surfaces of A) GIC, B) NGIC0, C) NGIC1, D) NGIC2, E) NGIC5. Energy dispersive X-ray spectra (right) of F) GIC, G) NGIC0, H) NGIC1, I) NGIC2, J) NGIC5. No silver peak in NGIC0 and GIC. *GIC, glass ionomer cement (GIC). NGIC0, GIC with 10% poly(vinylphosphonic acid)(PVPA) solid by weight. NGIC1, GIC with 1% Ag45S5 bioactive glass (NanoAg BAG) and 10% PVPA solid by weight. NGIC2, GIC with 2% NanoAg BAG and 10% PVPA solid by weight. NGIC5, GIC with 5% NanoAg BAG and 10% PVPA solid by weight.*

characterized by the adsorption peaks at 940 cm^{-1} and 1030 cm^{-1}. This is due to the fluoroaluminosilcate glass powder component after setting. The C═O symmetric and asymmetric vibrations are characterized by the adsorption peaks at 1400 cm^{-1} and 1458 cm^{-1}. This is associated with the polyacrylic acid liquid component after setting. The ionized COO- stretching vibration is characterized by the adsorption peaks at 1550 cm-1 which is due to the formation of salts of polyacrylic acid (PAA) with fluoroaluminosilcate glass powder ($PAA^-\_\_Ca^{2+}$ and $PAA^-\_\_Al^{3+}$) after setting. The C═O carbonyl stretching vibration (COOH) is characterized by the adsorption peak at 1700 cm^{-1} which is associated with polyacrylic acid that unionized after setting. The asymmetric and symmetric C-H stretching vibrations are characterized by the adsorption peaks at 2800 and 2900 cm^{-1} from polyacrylic acid after setting. The -OH hydroxyl stretching vibration is characterized by adsorption peak between 3200 and 3500 cm^{-1}.

3.6. Mechanical properties of NGIC

3.6.1. Compressive strength

Fig. 9A shows the compressive strength in MPa of the NGIC and GIC specimens. The mean compressive strength and SD of GIC, NGIC0, NGIC1, NGIC2 and NGIC5 were 168.13 ± 29.72 MPa, 205.51 ± 29.48 MPa, 221.77 ± 46.79 MPa, 216.61 ± 59.26 MPa and 167.69 ± 36.44 MPa, respectively. NIGC0, NGIC1 and NGIC2 groups exhibited higher compressive strength than GIC ($p < 0.01$); and NGIC1 have the highest compressive strength among all the groups ($p < 0.05$).

3.6.2. Diametral tensile strength

Fig. 9B showed the diametral tensile strength of various NGIC and GIC groups. The mean diametral tensile strength and SD of GIC, NGIC0, NGIC1, NGIC2 and NGIC5 was 14.14 ± 1.67 MPa, 18.27 ± 4.88 MPa, 21.15 ± 2.21 MPa, 17.23 ± 3.83 MPa and 13.33 ± 3.32 MPa, respectively. The NGIC2, NGIC1 and NGIC0 group showed higher diametral tensile strength than GIC ($p < 0.01$). NGIC1 have the highest diametral tensile strength among all groups. (**$p < 0.01$).

3.7. Ion release properties of NGIC

Fig. 10 shows release of fluoride (A), phosphate (B), calcium (C) and silver ions of the NGICs for 4 weeks.

3.7.1. Fluoride ions

The mean and SD of accumulative fluoride release in GIC, NGIC0, NGIC1, NGIC2 and NGIC5 after 4 weeks were 32.69 ± 0.93 mg/L, 32.74 ± 1.71 mg/L, 46.14 ± 4.04 mg/L, 50.79 ± 8.61 mg/L and 86.63 ± 8.36 mg/L, respectively (Fig. 10A). Fluoride release results showed that NGIC5 had the highest fluoride release. NGIC1, NGIC2 and NGIC5 had significantly higher fluoride release than GIC group ($p < 0.05$). The release of fluoride in NGIC0 group was similar to that of GIC ($p > 0.05$).

3.7.2. Phosphate ions

The mean and SD of accumulative phosphate release in GIC, NGIC0, NGIC1, NGIC2 and NGIC5 after 4 weeks were 0.71 ± 0.03 mg/L, 0.64 ± 0.05 mg/L, 0.71 ± 0.08 mg/L, 1.15 ± 0.19 mg/L and 4.05 ± 1.21 mg/L, respectively (Fig. 10B). Phosphate release results showed that NGIC5 had significantly higher phosphate release than other groups ($p < 0.05$). NGIC2 showed significantly higher phosphate release than GIC ($p < 0.05$). There was no statistical difference in phosphate release between NGIC0, NGIC1, and GIC ($p > 0.05$).

3.7.3. Calcium ions

The mean and SD of accumulative calcium release in GIC, NGIC0, NGIC1, NGIC2 and NGIC5 for 4 weeks were 0.00 ± 0.00 mg/L, 0.00 ± 0.00 mg/L, 0.00 ± 0.00 mg/L, 1.32 ± 0.26 mg/L and 3.11 ± 1.69 mg/L, respectively (Fig. 10C). Calcium release results showed that GIC, NGIC0 and NGIC1 had no detectable calcium release for 4 weeks ($p > 0.05$). NGIC2 and NGIC5 showed significantly higher calcium release than GIC ($p < 0.05$).

3.7.4. Silver ions

The mean and SD of accumulative silver release in GIC, NGIC0, NGIC1, NGIC2 and NGIC5 for 4 weeks were 0.00 ± 0.00 mg/L, 0.00 ± 0.00 mg/L, 0.01 ± 0.01 mg/L, 0.02 ± 0.01 mg/L and 0.07 ± 0.02 mg/L, respectively (Fig. 10D). Silver release results showed that the NGIC0 and GIC had no detectable silver release for 4 weeks. NGIC1, NGIC2 and NGIC5 showed increased silver release compared to GIC ($p < 0.05$), with NGIC5 having the highest silver release among all groups ($p < 0.05$).

4. Discussion

In this study, we have developed a novel glass ionomer material with significantly improved mechanical strength and ion release properties in this study. This NGIC has potential to be developed into restorative material, core materials, luting cement, and fissure sealant. NGICs exhibited significant improved mechanical strength compared with conventional GIC. The improved mechanical strength indicates a broaden clinical application in various site for restoration, including occlusal loading area. Moreover, NGICs release fluoride, and phosphate and silver sustainably and demonstrate a higher level of ion release compared to conventional GIC. The enhanced ion release of NGIC indicates its great potential in caries prevention and management in patients with dental caries, particularly for those at a high caries risk.

Our results indicated that the incorporation of PVPA at less than 10% weight percentage enhanced the mechanical strength of NGIC. NGIC incorporated with 10% PVPA showed the optimal effects. The addition and the weight percentage of PVPA affects the setting reaction of NGIC. During the setting reaction of NGIC, the ionization of PVPA releases H^+ ions and polyphosphonate. The H^+ ions attack the fluoroaluminosilicate glass surface in the powder component of NGIC and generate Na^+, Ca^{2+}, Al^{3+}, H_2PO^{4-} and F^- etc. ions into the aqueous phase. These ions form ionic crosslinks with polyphosphonate [32–34]. This setting reaction in NGIC is similar to the setting reaction of polyacrylic acid and fluoroaluminosilicate glass in the conventional GIC, in which the metal ions forms cross-link with polyacrylate [35]. The binding between metal ions such as Ca^{2+} and Al^{3+} and polyphosphonate are stronger than of polyacrylate [18]. The difference in the strength of the ionic crosslinks might explain the enhanced mechanical strength of NGIC compared to conventional GIC.

PVPA could not indefinitely enhance the mechanical strength. In this study, we found 20% PVPA significantly reduced the mechanical strength. The setting of NGIC involves mixing glass powder and liquid in the NGIC system. We mixed PVPA powder with the GIC liquid such that the PVPA was dissolved to form the solution. As the weight percentage of PVPA increased, the liquid viscosity increased. Mixing the glass powder and liquid with 20% PVPA became difficult due to insufficient wettability. Consequently, the setting reaction may have been incomplete. This could explain the reduced mechanical strength of NGIC with PVPA at higher weight percentages, as it may be attributable to an

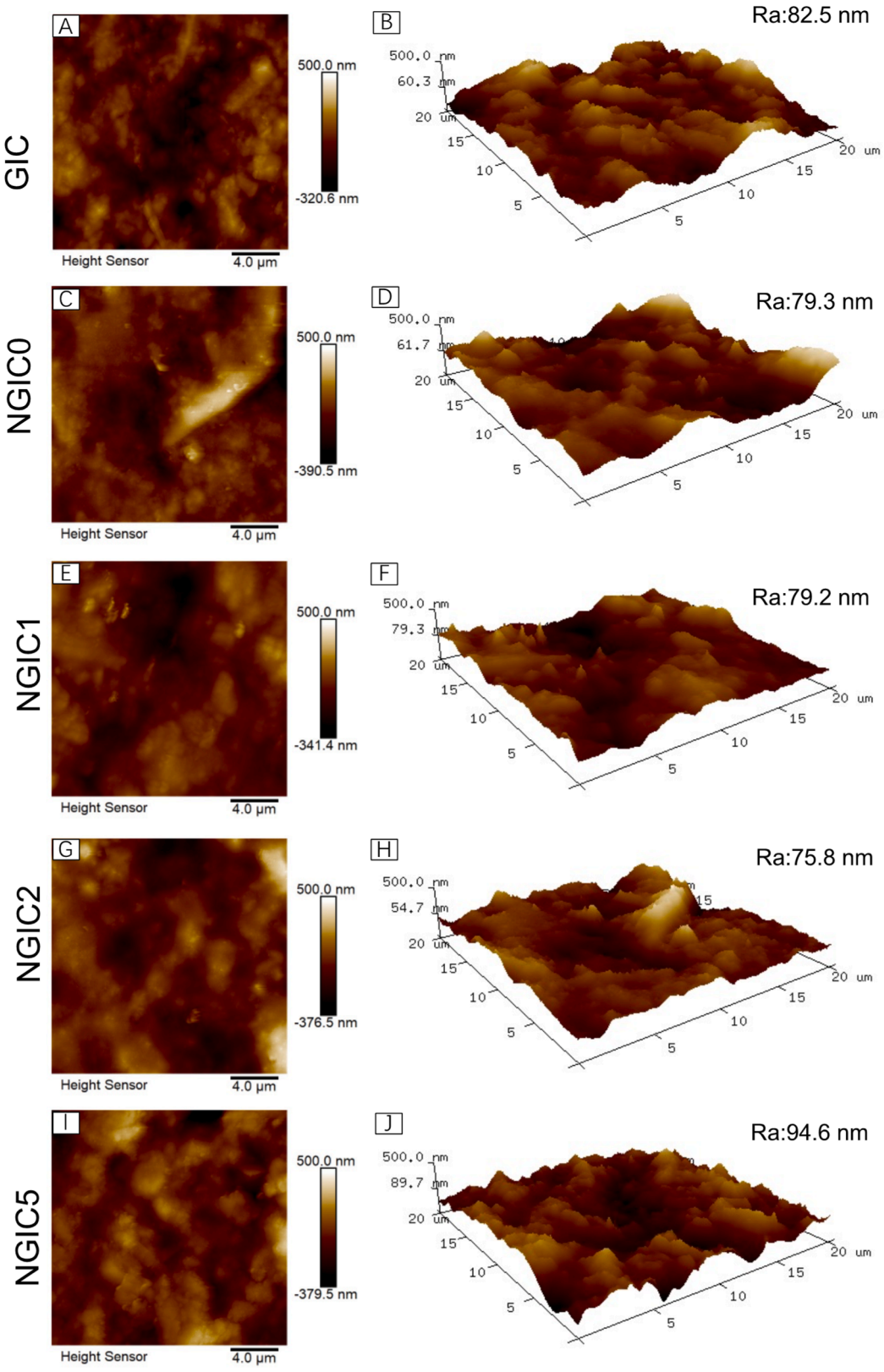

Fig. 7. Surface topography in 2D (left) and 3D (right) with surface roughness value in Ra of of novel glass ionomer cements (NGICs). Surface topography in 2D (left) had no observable difference of fracture surfaces of A) GIC, C) NGIC0, E) NGIC1, G) NGIC2, I) NGIC5. Surface topography in 3D (right) with surface roughness value in Ra of B) GIC, D) NGIC0, F) NGIC1, H) NGIC2, J) NGIC5. *GIC, glass ionomer cement (GIC). NGIC0, GIC with 10% poly(vinylphosphonic acid)(PVPA) solid by weight. NGIC1, GIC with 1% Ag45S5 bioactive glass (NanoAg BAG) and 10% PVPA solid by weight. NGIC2, GIC with 2% NanoAg BAG and 10% PVPA solid by weight. NGIC5, GIC with 5% NanoAg BAG and 10% PVPA solid by weight.*

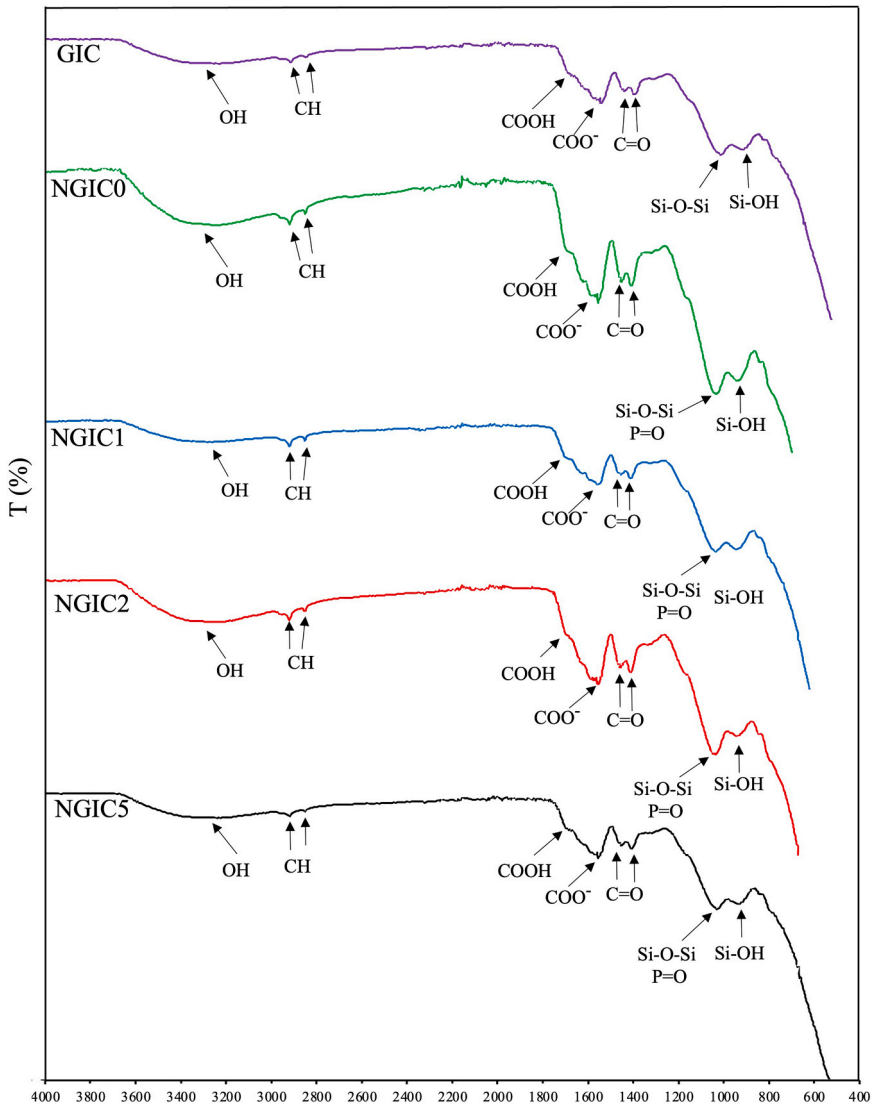

Fig. 8. The reprehensive FTIR spectra in various groups. *GIC, glass ionomer cement (GIC) NGIC0, GIC with 10% poly(vinylphosphonic acid)(PVPA) solid by weight. NGIC1, GIC with 1% Ag45S5 bioactive glass (NanoAg BAG) and 10% PVPA solid by weight. NGIC2, GIC with 2% NanoAg BAG and 10% PVPA solid by weight. NGIC5, GIC with 5% NanoAg BAG and 10% PVPA solid by weigh.*

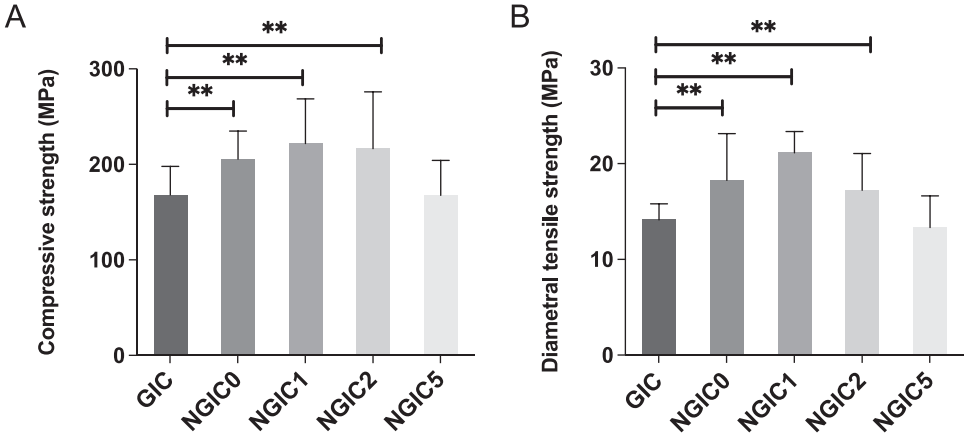

Fig. 9. The compressive strength (A) and diametral tensile strength (B) of NGIC specimens. GIC, glass ionomer cement (GIC). *NGIC0, GIC with 10% poly(vinylphosphonic acid)(PVPA) solid by weight. NGIC1, GIC with 1% Ag45S5 bioactive glass (NanoAg BAG) and 10% PVPA solid by weight. NGIC2, GIC with 2% NanoAg BAG and 10% PVPA solid by weight. NGIC5, GIC with 5% NanoAg BAG and 10% PVPA solid by weight.*

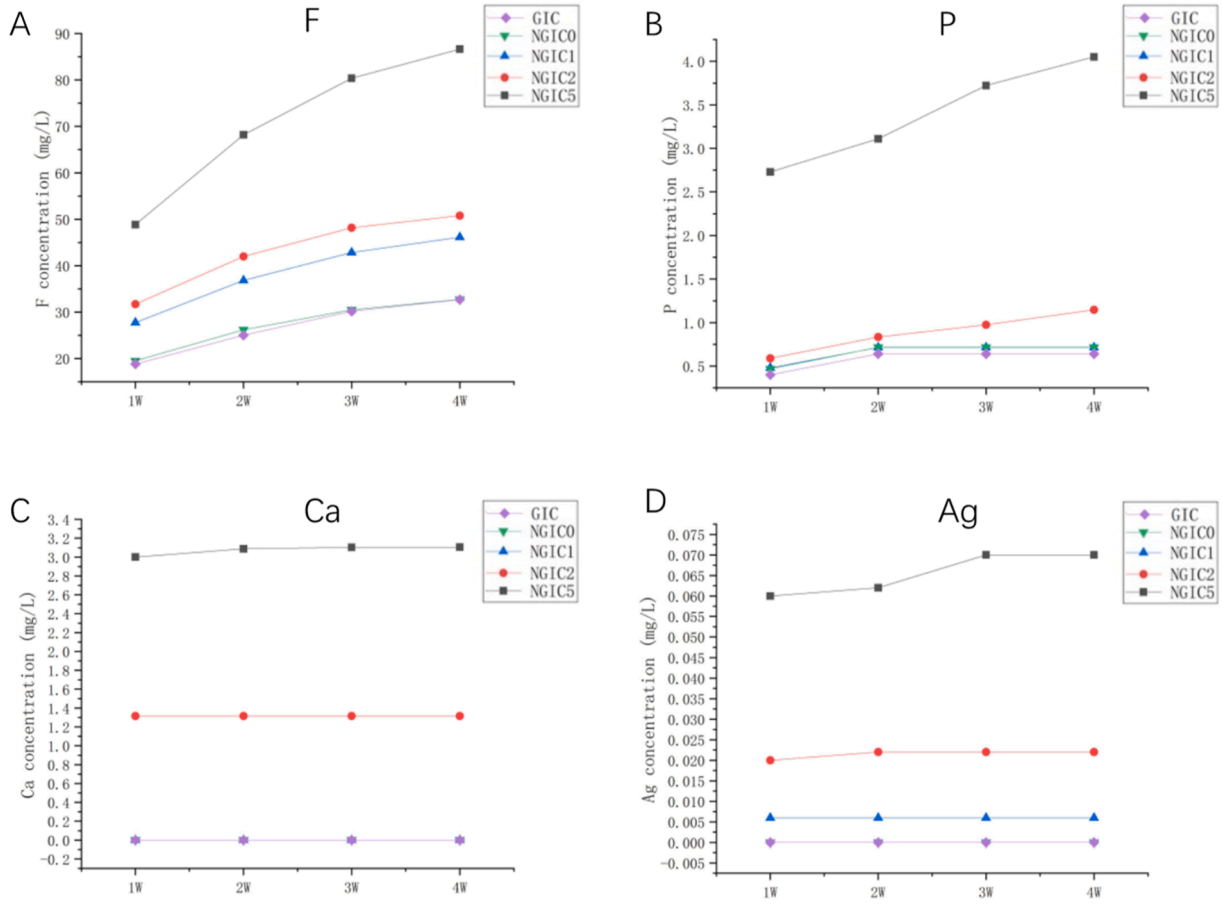

Fig. 10. The ion release in various group for 4 weeks. A) fluoride ion release; B) phosphate ion release; C) Calcium ion release; D) Silver ion release. *GIC, glass ionomer cement (GIC). NGIC0, GIC with 10% poly(vinylphosphonic acid)(PVPA) solid by weight. NGIC1, GIC with 1% Ag45S5 bioactive glass (NanoAg BAG) and 10% PVPA solid by weight. NGIC2, GIC with 2% NanoAg BAG and 10% PVPA solid by weight. NGIC5, GIC with 5% NanoAg BAG and 10% PVPA solid by weight.*

incomplete setting reaction.

The Ag nanoparticles (NPs) were incorporated into 45S5 bioactive glass (BAG). When the silver nitrate was added to the sol in the sol-gel process, the Ag NPs were generated from the thermal treatment of the dried gel at 700 °C for 3 h. The AgNO3 decomposes first into Ag_2O and then Ag at temperature higher than 440 °C ($AgNO_3 \rightarrow Ag_2O \rightarrow$ Ag NPs) [36]. The AgNPs were generated and distributed within the BAG matrix. The BAG can be used as a controlled drug delivery system in the case of Ag NPs [37]. The Ag NPs loaded BAG controls the release of Ag ions (Ag^0 NPs $\rightarrow Ag^+$) to inhibit the bacterial growth. The successful synthesis of the bioactive glass loaded with silver nanoparticles has been proved in two previous studies [38,39]. The Ag NPs were generated during the thermal treatment of bioactive glass gel after sol-gel process in both studies. Silver nitrate was also used to prepare the bioactive glass loaded with Ag NPs in the sol-gel process. The Ag nanoparticles were found to unevenly distribute within the BAG matrix [38], demonstrating the successful incorporation of Ag NPs into BAG matrix.

In this study, we found that incorporating 1% or 2% NanoAg BAG by weight significantly improved the mechanical strength of NGIC (Fig. 8). The addition of bioactive glass has the potential to enhance the mechanical strength of GIC, as it may provide strong interfacial bonding between the glass particles and the cement matrix [40]. However, we noted that the addition of BAG into glass ionomer or resin materials can negatively alter the mechanical strength of these materials in certain instances [20]. The impact of BAG on the mechanical properties of glass ionomer materials largely depends on the size of the BAG particles. Lohbauer et al. observed that incorporating smaller BAG particles (0.5–2 μm in diameter) into GIC showed higher compressive strength than the addition of larger BAG particles (4–8 μm in diameter) [41]. This was attributed to the more homogeneous and dense microstructure provided by the smaller BAG particles with increased surface area, thereby enhancing the cement's mechanical strength [41]. Consequently, we synthesized NanoAg BAG with particle diameter of approximately 50–150 nm (Fig. 1). The incorporation of 1% or 2% NanoAg BAG positively affected the mechanical strength of NGIC.

It is essential to ensure the biosafety of NGIC for clinical application by determining their biocompatibility. The incorporation and weight percentage of PVPA and NanoAg BAG might affect the biocompatibility of NGIC. In this study, NGIC with varying weight percentages of PVPA and 0% and 1% weight percentage of NanoAg BAG demonstrated similar biocompatibility to commercial GIC in cell toxicity tests for human gingival fibroblasts (Fig. 5). PVPA is a type of hydrophilic polymer with good biocompatibility [42], proven to be non-toxic and used as an additive in dental materials such as composites or electrospun membranes [43,44]. Our results also indicated that the addition of PVPA did not affect the biocompatibility of NGIC (Fig. 3).

NanoAg BAG exhibits a strong antimicrobial effect; however, it also presents increased cytotoxicity [45]. Therefore, we carried out cytotoxicity tests to determine the non-cytotoxic dose of NanoAg BAG in NGIC. The CCK-8 results demonstrated that NGIC1 exhibited similar biocompatibility to commercial conventional GIC. Conversely, NGIC2 and NGIC5 increased cytotoxicity compared to commercial conventional GIC, potentially due to the higher concentration of silver in NanoAg BAG in the NGIC. Phetnin et al. reported decreased cell viability with increasing silver content in BAG, which was consistent to our study [46]. Our results indicated that NGIC with 1% weight percentage of

NanoAg BAG exhibited the best biocompatibility, making it the optimal concentration for NGIC synthesis. Future studies on NGIC's clinical biosafety should be conducted to confirm the results of this in vitro study [47].

This study also examined the effects of adding PVPA and NanoAg BAG on the surface morphology and roughness of NGIC, which may be related to its mechanical and biological properties. We assessed the fractured surfaces of NGICs using SEM and found that their fractured surface morphology was similar to GIC (Fig. 6), indicating that the addition of NanoAg BAG and PVPA did not significantly impact the morphology of NGIC's fractured surface. Furthermore, AFM results revealed that the surface topography of NGICs was comparable to that of GIC (Fig. 7). NGICs with less than 2% NanoAg BAG displayed a slight decrease in surface roughness compared to GIC, although the differences were not statistically significant. However, NGIC5 exhibited increased surface roughness compared to GIC ($p < 0.05$).

The setting of NGIC was examined by FTIR. During the NGIC and GIC setting reaction, an ionization of -COOH group to COO- group of polyacrylic acid occurred during setting. The reaction of polyacrylic acid and glass powder formed the polyacrylate salt matrix and formation of ionic crosslinks [48]. Therefore, the adsorption at around 1550 cm^{-1}, i.e., ionization of COO^-, was more intense than the adsorption at 1700 cm^{-1} (-COOH) after 24 h setting. In GIC group, the Si-OH and Si-O-Si stretching vibrations were associated with the fluoroaluminosilcate glass powder component after setting. On the other hand, in NGIC1, NGIC2 and NGIC5 groups, the Si-OH and Si-O-Si stretching vibrations were associated with the fluoroaluminosilcate glass powder component and 45 S silver bioactive glass, and the P = O stretching vibrations were associated from PVPA after setting. The adsorption peaks for Si-OH and Si-O-Si functional groups and P = O were overlap with each other. The P = O stretch of the phosphonic acid side group appear between 1090 and 905 cm^{-1} [49], proving the setting reaction of PVPA with GIC.

We developed the NGIC primarily for caries prevention and management. The potential of NGIC for caries management were assessed by the release of the ions related to caries prevention and control, including fluoride, phosphate, calcium and silver ions. Fluoride can prevent demineralisation and promote remineralisation of dental hard tissue [50]. It is a common active ingredient of agents for caries prevention and management. Calcium and phosphate are the essential elements of hydroxyapatite, the main component of dental hard tissue [50,51]. Supplementing phosphate and calcium ions into the tooth surface might promote reminealisation of the demineralised tooth tissue and prevent caries progress, especially in the area where the saliva cannot reach [52]. Silver has antimicrobial effect and could prevent caries by inhibiting the growth of the cariogenic bacteria, thus is used for caries management [53]. Although further studies are needed, the release level of fluoride, phosphate, calcium and silver by NGIC may potentially reflect its effect on prevention and management of caries [54,55].

This study revealed that NGICs release fluoride sustainably for over 4 weeks, and the fluoride release was significantly higher than conventional GIC (Fig. 10A). Conventional GIC have caries preventive effect compared to other restorative materials though the effect was not satisfactory [56]. The caries preventive effect of conventional GIC is mainly due to their sustainable fluoride-releasing properties. NGIC presented a higher level of fluoride release, which may indicate a stronger caries preventive effect compared to GICs.

The results of calcium and phosphate release showed that NGICs with more than 2% weight percentage of NanoAg BAG released more calcium and phosphate ion compared to conventional GIC. It proved that the addition of NanoAg BAG enhanced the calcium and phosphate ion release of NGIC. However, calcium and phosphate release were not detected in NGIC with 1% or lower weight percentage of NanoAg BAG and GIC. Because GIC contains CaF_2 and $AlPO_4$ it was supposed to release calcium and phosphate when fluoride release was detected. In addition, NanoAg BAG also contributed to the calcium and phosphate release as proved in the ion release assessment of the NGIC 2 and NGIC 5 groups. Therefore, the released calcium and phosphate ion by GIC, NGIC0 and NGIC1 might be under the detectable threshold of ICT-OES and did not present a trackable result.

The result of silver release revealed that NGIC released a low level of silver while the commercial GIC have no silver release. The silver release of NGICs was not sustainable and depleted at various timepoints with different weight percentage of NanoAg BAG. The accumulative silver release was 0.00625 ug/cm^3 from NGIC with 1% NanoAg BAG, which is the optimal weight percentage. The amount of silver was substantially lower than the dose of the silver inhibiting cell growth [57]. Although the level of silver release was low, NGICs were considered to be antimicrobial because the silver incorporated into the NGICs might inhibit the growth of microorganism on or around the material, which need to be confirmed in future studies.

This study focused on the development of NGIC and the assessment of its mechanical properties and ion-releasing kinetics. The results showed promising result in developing a cost-effective material for effective caries prevention and management. Further assessment of physical, chemical and adhesive properties should be performed before the determination on the optimum composition of NGIC. In addition, further studies on its antimicrobial and remineralizing effect should be conducted to assess its potential on caries management.

5. Conclusion

We have developed a novel glass ionomer material which is biocompatible and with improved mechanical properties compared to conventional GIC. It presented enhanced fluoride, calcium, phosphate and silver ion release compared to conventional GIC.

Declaration of Competing Interest

The authors state that they have no conflict of interest.

References

[1] Hoshika S, Ting S, Ahmed Z, Chen F, Toida Y, Sakaguchi N, et al. Effect of conditioning and 1 year aging on the bond strength and interfacial morphology of glass-ionomer cement bonded to dentin. Dent Mater 2021;37:106–12.
[2] Agha A, Parker S, Patel MP. Development of experimental resin modified glass ionomer cements (RMGICs) with reduced water uptake and dimensional change. Dent Mater 2016;32:713–22.
[3] Global oral health status report: towards universal health coverage for oral health by 2030. Geneva: World Health Organization; 2022. Licence: CC BY-NC-SA 3.0 IGO.
[4] Kassebaum N, Smith A, Bernabé E, Fleming T, Reynolds A, Vos T, et al. Global, regional, and national prevalence, incidence, and disability-adjusted life years for oral conditions for 195 countries, 1990-2015: a systematic analysis for the global burden of diseases, injuries, and risk factors. J Dent Res 2017;96:380–7.
[5] Frencken JE, Peters MC, Manton DJ, Leal SC, Gordan VV, Eden E. Minimal intervention dentistry for managing dental caries - a review: report of a FDI task group. Int Dent J 2012;62:223–43.
[6] Banerjee A, Frencken J, Schwendicke F, Innes N. Contemporary operative caries management: consensus recommendations on minimally invasive caries removal. Br Dent J 2017;223:215–22.
[7] Torres PJ, Phan HT, Bojorquez AK, Garcia-Godoy F, Pinzon LM. Minimally invasive techniques used for caries management in dentistry. a review. J Clin Pedia Dent 2021;45:224–32.
[8] Ge KX, Lung CY, Lam WY, Chu CH, Yu OY. A novel glass ionomer cement with silver zeolite for restorative dentistry. J Dent 2023;133:1–13.
[9] Friedl K, Hiller KA, Friedl KH. Clinical performance of a new glass ionomer based restoration system: a retrospective cohort study. Dent Mater 2011;27:1031–7.
[10] Wiegand A, Buchalla W, Attin T. Review on fluoride-releasing restorative materials—Fluoride release and uptake characteristics, antibacterial activity and influence on caries formation. Dent Mater 2007;23:343–62.
[11] Hussainy SN, Nasim I, Thomas T, Ranjan M. Clinical performance of resin-modified glass ionomer cement, flowable composite, and polyacid-modified resin composite in noncarious cervical lesions: One-year follow-up. J Conserv Dent 2018;21:1–12.
[12] Lezaja Zebic M, Jakovljevic N, Miletic V. Fluoride release from conventional, resin-modified and hybrid glass ionomer cements. Serb Dent J 2018;65:187–94.
[13] Abueva CD, Lee B-T. Poly (vinylphosphonic acid) immobilized on chitosan: a glycosaminoglycan-inspired matrix for bone regeneration. Int J Biol Macromol 2014;64:294–301.

[14] Abbasi R, Nodehi A, Atai M. Synthesis of poly(acrylic-co-itaconic acid) through precipitation photopolymerization for glass-ionomer cements: Characterization and properties of the cements. Dent Mater 2020;36:169–83.
[15] Zhang C, Liu Y, Wen S, Wang S. Poly (vinylphosphonic acid)(PVPA) on titanium alloy acting as effective cartilage-like superlubricity coatings. ACS Appl Mater Interfaces 2014;6:71–8.
[16] Brunklaus G, Schauff S, Markova D, Klapper M, Müllen K, Spiess HW. Proton mobilities in phosphonic acid-based proton exchange membranes probed by 1H and 2H solid-state NMR spectroscopy. J Phys Chem B 2009;113:6674–81.
[17] Steininger H, Schuster M, Kreuer KD, Kaltbeitzel A, Bingöl B, Meyer WH, et al. Intermediate temperature proton conductors for PEM fuel cells based on phosphonic acid as protogenic group: a progress report. Phys Chem Chem Phys 2007;9:1764–973.
[18] Rivas BL, Pereira E, Gallegos P, Homper D, Geckeler KE. Metal ion binding capability of the water-soluble poly (vinyl phosphonic acid) for mono-, di-, and trivalent cations. J Appl Polym Sci 2004;92:2917–22.
[19] Khouw-Liu VHW, Anstice HM, Pearson GJ. An in vitro investigation of a poly(vinyl phosphonic acid) based cement with four conventional glass-ionomer cements. Part 1: flexural strength and fluoride release. J Dent 1999;27:351–7.
[20] Skallevold HE, Rokaya D, Khurshid Z, Zafar MS. Bioactive glass applications in dentistry. Int J Mol Sci 2019:20–44.
[21] Rahaman MN, Day DE, Bal BS, Fu Q, Jung SB, Bonewald LF, et al. Bioactive glass in tissue engineering. Acta Biomater 2011;7:2355–73.
[22] Vallittu PK. Bioactive glass-containing cranial implants: an overview. J Mater Sci 2017;52:8772–84.
[23] Hench LL. The story of Bioglass®. J Mater Sci: Mater Med 2006;17:967–78.
[24] Banerjee A, Pabari H, Paolinelis G, Thompson ID, F Watson T. An in vitro evaluation of selective demineralised enamel removal using bio-active glass air abrasion. Clin Oral Invest 2011;15:895–900.
[25] Drago L, Vecchi ED, Bortolin M, Toscano M, Mattina R, Romanò CL. Antimicrobial activity and resistance selection of different bioglass S53P4 formulations against multidrug resistant strains. Future Microbiol 2015;10:1293–9.
[26] Espinosa-Cristóbal LF, Holguín-Meráz C, Zaragoza-Contreras EA, Martínez-Martínez RE, Donohue-Cornejo A, Loyola-Rodríguez JP, et al. Antimicrobial and substantivity properties of silver nanoparticles against oral microbiomes clinically isolated from young and young-adult patients. J Nanomater 2019;2019:1–14.
[27] Yin IX, Yu OY, Zhao IS, Mei ML, Li QL, Tang J, et al. Inhibition of dentine caries using fluoride solution with silver nanoparticles: An in vitro study. J Dent 2020;103:1–7.
[28] Makanjuola J, Deb S. Chemically activated glass-ionomer cements as bioactive materials in dentistry: a review. Prosthesis 2023;5:327–45.
[29] Pirayesh H, Nychka JA. Sol–gel synthesis of bioactive glass-ceramic 45S5 and its in vitro dissolution and mineralization behavior. J Am Ceram Soc 2013;96:1643–50.
[30] Yamakami SA, Ubaldini ALM, Sato F, Medina Neto A, Pascotto RC, Baesso ML. Study of the chemical interaction between a high-viscosity glass ionomer cement and dentin. J Appl Oral Sci 2018;26:1–13.
[31] Valliant E, Dickey B, Price R, Boyd D, Filiaggi M. Fourier transform infrared spectroscopy as a tool to study the setting reaction in glass-ionomer cements. Mater Lett 2016;185:256–9.
[32] Greish Y, Brown P. Chemically formed HAp-Ca poly (vinyl phosphonate) composites. Biomater 2001;22:807–16.
[33] Greish Y, Brown P. Preparation and characterization of calcium phosphate-poly (vinyl phosphonic acid) composites. J Mater Sci: Mater Med 2001;12:407–11.
[34] Greish YE, Brown PW. Formation and properties of hydroxyapatite–calcium poly (vinyl phosphonate) composites. J Am Ceram Soc 2002;85:1738–44.
[35] Nicholson JW. Chemistry of glass-ionomer cements: a review. Biomater 1998;19:485–94.
[36] Lara HH, Romero-Urbina DG, Pierce C, Lopez-Ribot JL, Arellano-Jiménez MJ, Jose-Yacaman M. Effect of silver nanoparticles on Candida albicans biofilms: an ultrastructural study. J Nanobiotechnology 2015;13:1–12.
[37] Gupta S, Majumdar S, Krishnamurthy S. Bioactive glass: A multifunctional delivery system. J Control Release 2021;335:481–97.
[38] Yang TY, Chern GI, Wang WH, Shih CJ. Synthesis, Characterization, and bioactivity of mesoporous bioactive glass codoped with zinc and silver. Int J Mol Sci 2023;24:1–19.
[39] Sánchez-Salcedo S, García A, González-Jiménez A, Vallet-Regí M. Antibacterial effect of 3D printed mesoporous bioactive glass scaffolds doped with metallic silver nanoparticles. Acta Biomater 2023;155:654–66.
[40] De Caluwe T, Vercruysse CWJ, Ladik I, Convents R, Declercq H, Martens L, et al. Addition of bioactive glass to glass ionomer cements: Effect on the physico-chemical properties and biocompatibility. Dent Mater 2017:186–203.
[41] Lohbauer U, Krämer N, Siedschlag G, Schubert EW, Lauerer B, Müller FA, et al. Strength and wear resistance of a dental glass-ionomer cement with a novel nanofilled resin coating. Am J Dent 2011;24:124–38.
[42] Cai H, Zhang C, Li F, Liu M, Zhang T, Chu H, et al. Study on the microcosmic superlubricity mechanism of PVPA affected by metal cations. Friction 2023;11:1150–64.
[43] Greish YE, Brown PW. Chemically formed HAp-Ca poly(vinyl phosphonate) composites. Biomater 2001;22:807–16.
[44] Franco RA, Sadiasa A, Lee BT. Utilization of PVPA and its effect on the material properties and biocompatibility of PVA electrospun membrane. Polym Adv Technol 2014;25:55–65.
[45] Akter M, Sikder MT, Rahman MM, Ullah AKMA, Hossain KFB, Banik S, et al. A systematic review on silver nanoparticles-induced cytotoxicity: Physicochemical properties and perspectives. J Adv Res 2018;9:1–16.
[46] Phetnin R, Rattanachan ST. Preparation and antibacterial property on silver incorporated mesoporous bioactive glass microspheres. J Solgel Sci Technol 2015;75:279–90.
[47] Hatton PV, Hurrell-Gillingham K, Brook IM. Biocompatibility of glass-ionomer bone cements. J Dent 2006;34:598–601.
[48] Sidhu SK, Nicholson JW. A Review of Glass-Ionomer Cements for Clinical Dentistry. J Funct Biomater 2016;7:1–16.
[49] Dey R, Wimpenny I, Gough J, Watts D, Budd P. Poly(vinylphosphonic acid- co -acrylic acid) hydrogels: The effect of copolymer composition on osteoblast adhesion and proliferation. J Biomed Mater Res A 2017;106:8638–47.
[50] Arifa MK, Ephraim R, Rajamani T. Recent advances in dental hard tissue remineralization: a review of literature. Int J Clin Pediatr Dent 2019;12:139–44.
[51] Kantharia N, Naik S, Apte S, Kheur M, Kheur S, Kale B. Nano-hydroxyapatite and its contemporary applications. Bone 2014;34:15–9.
[52] Abou Neel EA, Aljabo A, Strange A, Ibrahim S, Coathup M, Young AM, et al. Demineralization-remineralization dynamics in teeth and bone. Int J Nanomed 2016;11:4743–63.
[53] Nizami MZI, Xu VW, Yin IX, Yu OY, Chu CH. Metal and metal oxide nanoparticles in caries prevention: a review. Nanomater (Basel) 2021;11:1–13.
[54] Zhao IS, Mei ML, Burrow MF, Lo EC, Chu CH. Prevention of secondary caries using silver diamine fluoride treatment and casein phosphopeptide-amorphous calcium phosphate modified glass-ionomer cement. J Dent 2017;57:38–44.
[55] Ten Cate J. Review on fluoride, with special emphasis on calcium fluoride mechanisms in caries prevention. E Eur J Oral Sci 1997;105:461–5.
[56] Ge KX, Quock R, Chu CH, Yu OY. The preventive effect of glass ionomer restorations on new caries formation: A systematic review and meta-analysis. J Dent 2022;125:1–12.
[57] Loo YY, Rukayadi Y, Nor-Khaizura M-A-R, Kuan CH, Chieng BW, Nishibuchi M, et al. In vitro antimicrobial activity of green synthesized silver nanoparticles against selected gram-negative foodborne pathogens. Front Microbiol 2018;9:1–7.